



Fanconi anemia signaling network regulates the spindle assembly checkpoint

Grzegorz Nalepa,¹ Rikki Enzor,^{1,2} Zejin Sun,¹ Christophe Marchal,¹ Su-Jung Park,¹ Yanzhu Yang,¹ Laura Tedeschi,¹ Stephanie Kelich,¹ Helmut Hanenberg,^{1,3,4} and D. Wade Clapp^{1,2,4,5}

¹Department of Pediatrics, Herman B Wells Center for Pediatric Research, and ²Department of Microbiology and Immunology, Indiana University School of Medicine, Indianapolis, Indiana, USA. ³Department of Otorhinolaryngology (ENT), Heinrich Heine University School of Medicine, Düsseldorf, Germany. ⁴Department of Medical and Molecular Genetics and ⁵Department of Biochemistry and Molecular Biology, Indiana University School of Medicine, Indianapolis, Indiana, USA.

Fanconi anemia (FA) is a heterogenous genetic disease with a high risk of cancer. The FA proteins are essential for interphase DNA damage repair; however, it is incompletely understood why FA-deficient cells also develop gross aneuploidy, leading to cancer. Here, we systematically evaluated the role of the FA proteins in chromosome segregation through functional RNAi screens and analysis of primary cells from patients with FA. We found that FA signaling is essential for the spindle assembly checkpoint and is therefore required for high-fidelity chromosome segregation and prevention of aneuploidy. Furthermore, we discovered that FA proteins differentially localize to key structures of the mitotic apparatus in a cell cycle-dependent manner. The essential role of the FA pathway in mitosis offers a mechanistic explanation for the aneuploidy and malignant transformation known to occur after disruption of FA signaling. Collectively, our findings provide insight into the genetically unstable cancers resulting from inactivation of the FA/BRCA pathway.

Introduction

Fanconi anemia (FA) is a genetic disorder resulting from germline mutations in 1 out of 15 known FA or FA-like genes (*FANCA-FANCP*) (1–3). In addition to bone marrow failure and congenital malformations, patients with FA develop various malignancies, including acute leukemias and squamous cell carcinomas (4, 5). Mutations in the FA network are etiologically implicated in a significant proportion of inherited breast, pancreatic, and ovarian cancers (6–12). The high risk of malignant transformation in FA-deficient cells is due to genomic instability characterized by impaired DNA repair, chromosome breakage, and gross aneuploidy (13–15). Although the role of FA signaling in interphase DNA cross-link repair is well established (5, 16), the origins of gross aneuploidy in FA-deficient cells are incompletely understood.

The spindle assembly checkpoint (SAC) is the tumor suppressor signaling network that ensures high-fidelity chromosome segregation during mitosis to prevent aneuploidy (17, 18). It is established that FA-deficient cells have a high frequency of aneuploidy and micronucleation, which are symptoms of chromosome missegregation (13, 14, 19–23). However, the potential role of the FA pathway in the SAC has not been systematically analyzed. Our recent work in a genetically engineered murine model of FA that recapitulates the malignant hematopoietic manifestations of human FA (24) highlighted the correlation among gross aneuploidy, myelodysplasia, and leukemia in FA (14). Interestingly, we observed dysregulation of SAC proteins MAD2 and BUBR1 in this mouse model (D.W. Clapp, unpublished observations). Therefore, we hypothesized that the FA pathway may be essential for the SAC. Here we describe the results of comprehensive studies that address this hypothesis.

Results

Functional RNAi screen reveals role for FA signaling in the SAC. We generated an FA siRNA library against the 15 known human FA gene products and successfully validated these siRNAs via immunoblotting (Supplemental Figure 1, A–N; supplemental material available online with this article; doi:10.1172/JCI67364DS1). To examine the status of the SAC upon FA knockdown, we performed a functional RNAi screen as described previously (25, 26). HeLa cells were transfected with arrayed library siRNAs, challenged with taxol to activate the SAC through disruption of spindle microtubules, fixed, and imaged (Figure 1A). Negative control cells arrested in prometaphase due to SAC activation by taxol (Figure 1B). RNAi knockdown of the SAC regulator MAD2 resulted in multinucleation of taxol-treated cells due to SAC inactivation (Figure 1B and refs. 25, 26). Remarkably, we found that RNAi silencing of each FA gene except *FANCM* inactivated the SAC, as evidenced by multinucleation in response to taxol, similar to *MAD2* (Figure 1, C and D, and Supplemental Figure 2, A and B). Off-target siRNA effects are a risk in mitotic RNAi screens, and *MAD2* has been shown to be particularly susceptible (27). Thus, for each of the FA proteins identified as SAC regulators in the screen, we performed immunoblotting to show that *MAD2* is not nonspecifically knocked down by FA siRNAs (Supplemental Figure 3, A–J) or tested multiple unique siRNA sequences targeting each FA gene product (Supplemental Figure 1, A–D). When multiple siRNAs were tested, the severity of SAC failure correlated with the degree of target protein knockdown (Supplemental Figure 1, A–D). Since patients with FA frequently develop aneuploidy-associated hematopoietic malignancies (4, 28), we tested whether the FA pathway controls the SAC in primary hematopoietic cells. Indeed, shRNA knockdown of *FANCA* disrupted the SAC in primary human CD34⁺ cells, as shown by microscopy-coupled flow cytometry analysis (Figure 2). When treated with taxol, cycling *FANCA*-knockdown CD34⁺ cells became multinucleated (Figure 2 and Supplemental Figure 4). These data support the hypothesis that FA signaling is essential for the human SAC.

Authorship note: Grzegorz Nalepa and Rikki Enzor contributed equally to this work.

Conflict of interest: The authors have declared that no conflict of interest exists.

Citation for this article: *J Clin Invest.* 2013;123(9):3839–3847. doi:10.1172/JCI67364.

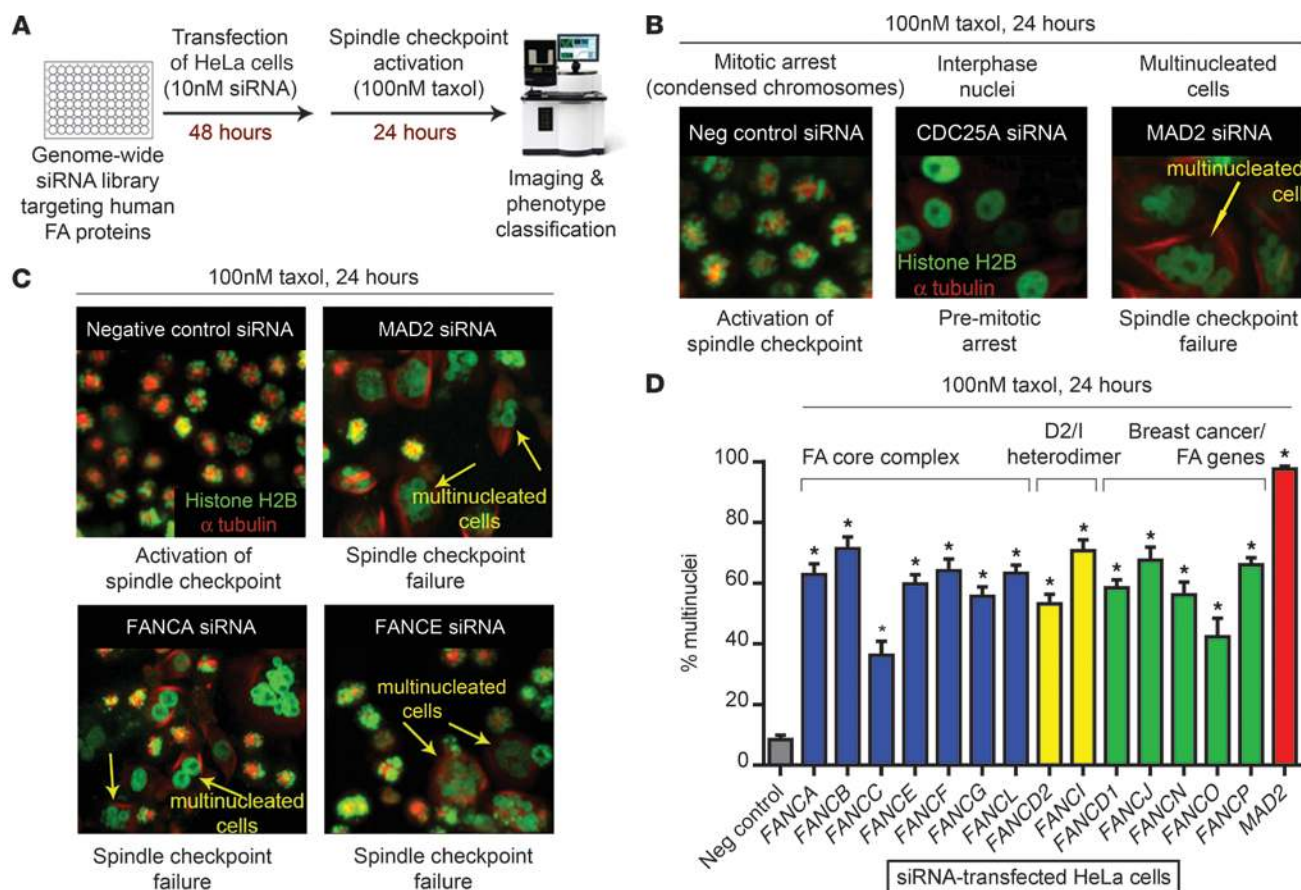


Figure 1
 FA signaling is essential for the SAC. **(A)** RNAi screen schematic. **(B)** Microscopy-based screen readout. HeLa^{GFP-H2B/mCherry-αtubulin} cells arrest in prometaphase upon taxol exposure. CDC25A knockdown results in premitotic arrest (25). MAD2 siRNA induces multinucleation due to SAC failure. Original magnification, ×200 (BD Pathway 855). **(C)** Representative images of cells transfected with indicated siRNAs and treated with taxol. Note multinucleation induced by FANCA and FANCC siRNAs and MAD2 siRNA (positive control). Original magnification, ×200 (BD Pathway 855). **(D)** Quantification of screen results. *P < 0.0001 (1-way ANOVA); n = 9 counts per siRNA. All bars represent mean values ± SEM.

Spindle checkpoint failure in cells from patients with FA. To validate the RNAi screen, we tested SAC activity in primary fibroblasts isolated from patients with FA of all available (12 out of 15) FA complementation groups (Figure 3A and see Supplemental Table 1 for list of FA mutations). Consistent with the RNAi screen results, primary fibroblasts of all tested FA complementation groups became multinucleated in response to taxol, while fibroblasts obtained from healthy individuals arrested in prometaphase (Figure 3, B and C; Supplemental Figure 5; and Supplemental Figure 6A). We confirmed SAC failure in primary FA cells using quantitative flow cytometry (Supplemental Figure 6D). Importantly, stable expression of the missing FANCA protein in primary FA-A fibroblasts not only rescued hypersensitivity to mitomycin known to result from loss of FA signaling (Supplemental Figure 7), but also the SAC failure following exposure to taxol (Figure 3D and Supplemental Figure 6B). We also found that FANCA is required for mitotic arrest in response to nocodazole, another spindle poison that is mechanistically different from taxol (Figure 3E and Supplemental Figure 6C). Collectively, these findings confirm an essential role for FA signaling in the human SAC using primary cells from patients with FA.

FA proteins localize to mitotic spindle and centrosomes during cell division. We then asked whether FA proteins localize to the mitotic apparatus in a cell cycle-dependent manner, which would be predicted based on their newly found role in the SAC (Figures 1–3). We found that 8 FA proteins (FANCA, FANCB, FANCE, FANCG, FANCL, FANCD1, FANCD2, and FANCN, also known as PALB2) localize to centrosomes during mitosis. We validated this finding by high-resolution immunofluorescence of 7 endogenous FA proteins (FANCA, FANCB, FANCE, FANCG, FANCN, FANCD2, and FANCD1) and 2 GFP-fused FANCG and FANCL proteins (Figure 4, A, C, and D; Supplemental Figures 8 and 9; and G. Nalepa, R. Enzor, and D.W. Clapp, unpublished observations). Additionally, FANCC and, to a lesser degree, FANCA localized to the mitotic spindle in a cell cycle-dependent manner (Figure 4, A and B, and Supplemental Figure 10). This experiment revealed that FA proteins are found on the mitotic apparatus during cell division (Figure 4D), consistent with a role for the FA pathway in the SAC.

Failure of centrosome maintenance in FA cells. Given the newly identified role of the FA pathway in mitosis (Figures 1–3) and centrosomal localization of multiple FA proteins (Figure 4 and Supplemental Figures 8 and 9), we questioned whether the FA network is function-

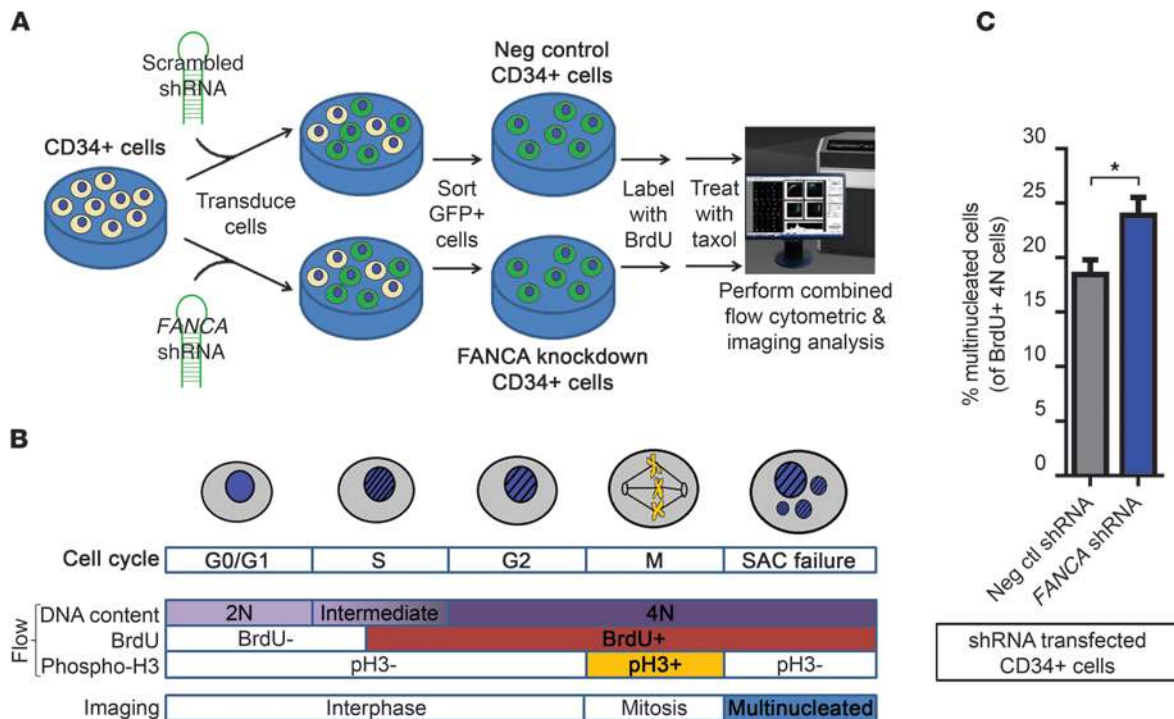


Figure 2 FANCA is essential for the SAC in primary human CD34+ cells. **(A)** CD34+ cell experiment schematic. **(B)** Microscopy-coupled flow cytometry allows quantification of SAC failure in cycling CD34+ cells. **(C)** Quantification of SAC failure in cycling FANCA shRNA–transduced CD34+ cells. **P* = 0.029 (2-tailed *t* test); *n* = 6. All bars represent mean values ± SEM.

ally important for maintenance of normal centrosome number (1 or 2 centrosomes per cell, depending on cell cycle stage). This question is clinically significant because extra centrosomes cause aneuploidy and cancer through promotion of merotelic kinetochore-spindle association (29). When we immunostained with endogenous pericentrin (a known centrosome marker) in FA cells, we found that primary fibroblasts from patients with FA contained abnormally high numbers of centrosomes compared with control fibroblasts (Figure 5, A, B, and D). We also noted structural nuclear abnormalities (multinucleated cells and micronuclei) in patient fibroblasts from all tested FA complementation groups cultured ex vivo without spindle poisons (Figure 5, C and E), consistent with previous reports (20–22, 30). We found that HeLa cells transfected with siRNAs against FA genes acquire extra centrosomes as well (Supplemental Figure 11, A and B). We concluded that FA-deficient cells accumulate supernumerary centrosomes. While a previous study suggested that one FA protein (FANCD1, also known as BRCA2) is critical for centrosome maintenance and localizes to centrosomes (15), our findings suggest that other FA proteins are also essential for maintaining normal centrosome numbers. Our preliminary experiments suggest that passage through mitosis is essential for centrosome accumulation in FA-deficient cells (G. Nalepa, R. Enzor, and D.W. Clapp, unpublished observations). Further work will be needed to validate this observation.

Discussion

The FA pathway, genomic instability, and cancer. The aneuploidy and multinucleation consistently observed in FA-deficient cells (20–23, 30) are suggestive of abnormal cell division (31), but the role of the FA

pathway in mitosis has previously not been well defined. Several publications revealed a biochemical interaction between FA proteins and the key mitotic cyclin-dependent kinase CDK1 (32, 33), while other work established an essential role for CDK1 in the SAC (34). A previous study in a murine model highlighted the functional cross-talk between the SAC pathway and FANCD1, a breast cancer tumor suppressor subsequently discovered to be an FA protein (35). Recently, it was proposed that some FA proteins resolve replication stress-induced chromatin bridges during anaphase (19, 20) and regulate cytokinesis (30). The data presented here, combined with these previous investigations, clearly demonstrate that abnormal cell division occurs in the absence of FA signaling. The SAC is a key tumor suppressor signaling network that protects cells from aneuploidy by ensuring accurate chromosome segregation, and SAC regulators have been implicated in a number of cancers (17, 18). Thus, we suggest that the newly discovered role for the FA signaling network in regulating the SAC (Figures 1–3) may contribute to the increased risk of aneuploidy and malignant transformation in FA-deficient cells.

Additionally, we hypothesize that error-prone mitosis may exacerbate mutagenesis resulting from disrupted DNA damage repair in FA-deficient cells. Recent elegant work showed that micronuclei generated through abnormal mitoses are sites of intense DNA breakage and mutagenesis, culminating in chromosome pulverization (36) and cancer (37). FA-deficient cells are prone to spontaneous multinucleation (Figure 5A; Supplemental Figure 11, C and E; and ref. 22), presumably due to a combination of weakened SAC (Figures 1–3), acquisition of supernumerary centrosomes (Figure 5 and Supplemental Figure 11), and failed cytokinesis (30). We pro-

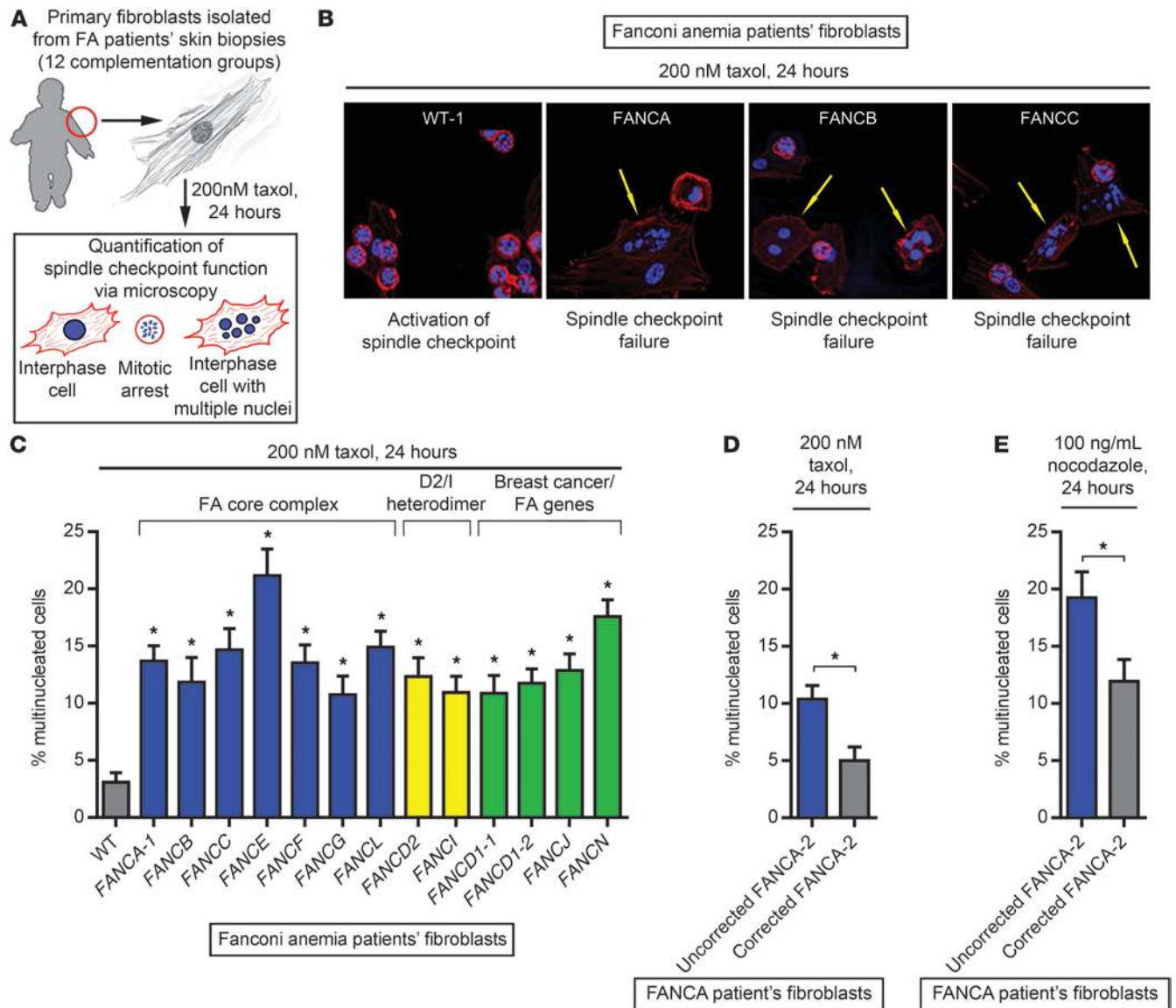


Figure 3 Spindle checkpoint failure in primary human FA cells. **(A)** Experiment schematic. **(B)** FA fibroblasts fail to arrest in mitosis upon taxol exposure and generate multinucleated cells (arrows). Original magnification, $\times 200$ (Applied Precision personalDX). **(C)** Quantification of SAC defects in cells from patients with FA. $*P < 0.01$ (1-way ANOVA with post-hoc Bonferroni's correction); $n = 10-15$ counts per genotype. **(D)** Ectopic expression of FANCA rescues the SAC defect in FA-A fibroblasts exposed to taxol. $*P = 0.0038$ (2-tailed t test); $n = 15$ counts. **(E)** FANCA-deficient patient fibroblasts fail to arrest at the SAC in response to nocodazole. $*P = 0.021$ (2-tailed t test); $n = 15$ counts. All bars represent mean values \pm SEM.

pose that DNA damage in the micronuclei of FA-deficient cells cannot be effectively resolved due to the crucial role of the FA pathway in interphase DNA damage repair (reviewed in ref. 2). Ultimately, this vicious cycle of abnormal cell division followed by multinucleation and mutagenesis may lead to cell death or genomic instability and transformation in FA-deficient cells (ref. 31 and Figure 6).

In summary, our study identifies a novel role for the FA signaling network in mitosis. The discovery of SAC failure in FA-deficient cells advances our understanding of chromosomal instability in patients with FA. As somatic inactivation of the FA pathway occurs in a spectrum of spontaneous malignancies, our studies are relevant to the pathogenesis and treatment of cancers in the general population.

Methods

Cell culture, siRNA library, and screen. HeLa cells, including HeLa cells stably expressing GFP- γ tubulin/GFP-CENPA (38) and HeLa cells stably expressing GFP-H2B/mCherry- α tubulin (39), were cultured in DMEM supplemented with 10% FBS and penicillin/streptomycin. Human skin fibroblasts from patients with FA and healthy controls were cultured at 5% oxygen in DMEM supplemented with 10% FBS, 1% glutamine, 1% sodium pyruvate, and penicillin/streptomycin. A customized Silencer Select siRNA library against all known FA proteins (coverage: at least 3 siRNAs per gene) was designed and ordered from Ambion/Life Technologies. A validated siRNA against MAD2 was used as a positive control, and the Negative Control siRNA #1 (Ambion) was used as a negative control. HeLa cells stably expressing GFP-H2B/mCherry- α tubulin (39) were reverse transfected

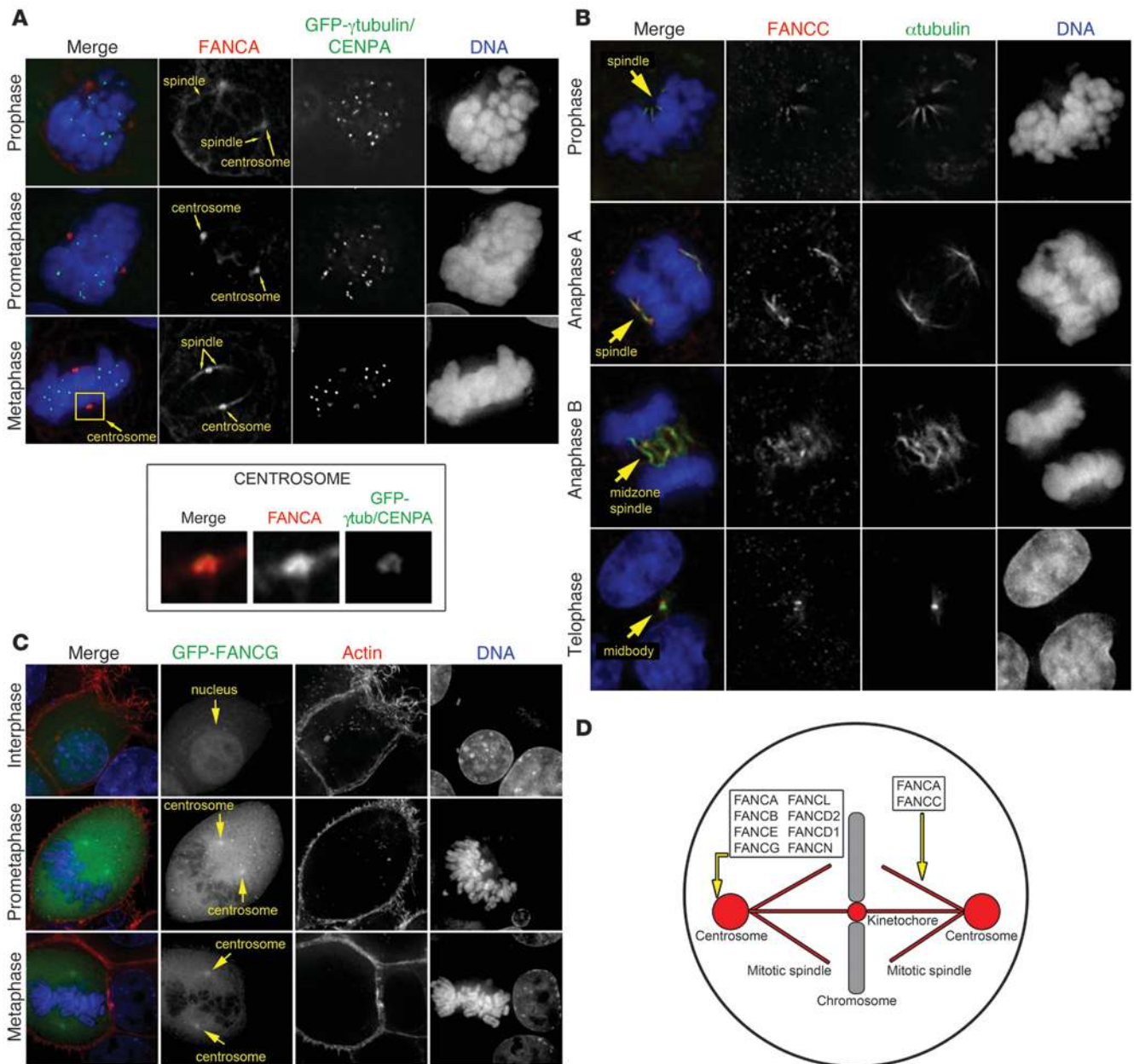


Figure 4

FA pathway proteins associate with centrosomes and mitotic spindle during cell division. **(A)** Endogenous FANCA and **(C)** GFP-FANCG localize to centrosomes during mitosis. Original magnification, $\times 1,000$ (Applied Precision personalDX). **(A)** A fraction of FANCA also localizes to the spindle, which emanates from the centrosomes during prophase and metaphase. **(B)** Endogenous FANCC colocalizes with α -tubulin at the spindle in early mitosis; midzone spindle during late anaphase; and midbody during telophase. Original magnification, $\times 1,000$ (Applied Precision personalDX). **(D)** Subcellular localization of FA proteins during mitosis.

with siRNA (10 nM) on 96-well plates (BD Falcon imaging microplates; 2,500 HeLa cells per well) using siPORT NeoFX transfection reagent (Applied Biosystems). After 48 hours, cells were exposed to 100 nM taxol for 24 hours and then fixed with 4% paraformaldehyde for imaging on the high-throughput automated screening microscope (BD Pathway 855, BD Biosystems). The initial screen was repeated with positive hit siRNAs (defined as $>20\%$ change compared with negative control-transfected cells) using a deconvolution microscope for cell imaging and counts. The following siRNAs were used for the repeat siRNA screen: FANCA (s162,

s163, s164, 120953, 105965, 7827), FANCB (s5012, s5013, s5014, s225863, s225864, 39216), FANCC (s4985), FANCE (s4992), FANCF (s5015), FANCG (s5018), FANCL (s30218), FANCM (s33619, s33620, s33621), FANCD2 (s4988), FANCI (s30461), FANCD1 (s2085), FANCI (also known as BRIP1) (s38384), FANCN (also known as PALB2) (s36198), FANCO (also known as RAD51C) (s11737, s11738, s11739), FANCP (also known as SLX4) (s39052, s39053, s39054), MAD2 (143483), and negative control (4390843) (all from Invitrogen). Mitotic nuclei, interphase nuclei, and multinuclei were quantified by manual counting using ImageJ software.

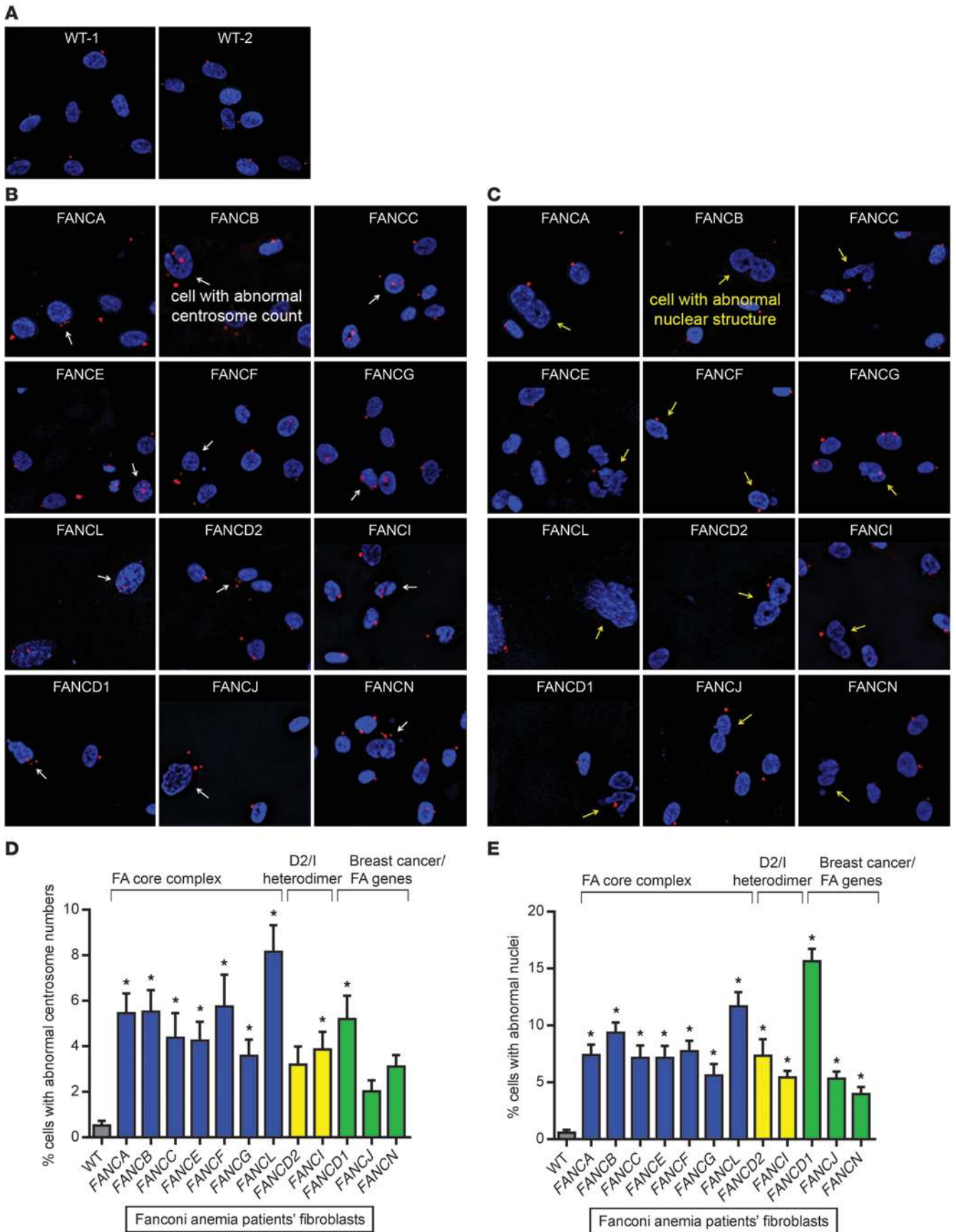




Figure 5

Abnormal centrosome counts and spontaneous micronucleation in cells of patients with FA. **(A)** Fibroblasts obtained from healthy controls contain 1–2 centrosomes per cell, as shown by endogenous pericentrin immunofluorescence (red). **(B)** Fibroblasts isolated from patients with FA contain supernumerary centrosomes (white arrows). **(C)** Fibroblasts from patients with FA have abnormal nuclear structures and undergo spontaneous micronucleation (yellow arrows). Original magnification, $\times 200$ (Applied Precision personalDX). **(D and E)** Increased fraction of cells with abnormal centrosome counts and abnormal nuclei in primary fibroblasts from patients with FA. * $P < 0.05$ compared with WT (1-way ANOVA with post-hoc Bonferroni's correction). All bars represent mean values \pm SEM.

Isolation of CD34⁺ human stem cells. Human umbilical cord blood was obtained from the In Vivo Therapeutics Core of the Indiana University Simon Cancer Center, and CD34⁺ human stem and progenitor cells were isolated by magnetic-activated cell sorting (MACS). Briefly, the low-density cells were separated from red blood cells by density centrifugation and by lysing the remaining red blood cells. The CD34⁺ cells were labeled with human CD34 antibody conjugated with magnetic microbeads (Miltenyi Biotec) and isolated with MACS separation column (Miltenyi Biotec).

FANCA shRNA knockdown and phenotypic characterization in ex vivo-cultured CD34⁺ cells. Human CD34⁺ primary cells (isolated as described above) were transduced with a GFP-tagged lentiviral construct containing either scrambled negative control shRNA or a combination of two shRNA sequences against FANCA (Z. Sun and H. Hanenberg, Indiana University, Indianapolis, Indiana, USA; unpublished observations) and cultured for 4 days at 5% oxygen in IMDM supplemented with 20% FBS, penicillin/streptomycin, 100 ng/ml SCF, 100 ng/ml TPO, and 100 ng/ml FLT3. The GFP-positive cells were sorted using a FACSCalibur flow cytometer and cultured overnight as described above. The cells were pulsed with 10 μ M BrdU for 4 hours and then treated with 100 nM taxol for 24 hours. Next, the cells were fixed, permeabilized, and stained with Hoechst 33342 DNA stain (Invitrogen), PE-conjugated antibody detecting phosphorylated histone H3 (Cell Signaling Technology), and APC-conjugated anti-BrdU according to the manufacturer's protocol for the BD Pharmingen APC-BrdU Kit. Finally, concurrent flow cytometry and imaging data were collected using an Amnis ImageStreamX Mark II imaging flow cytometer, and the data were analyzed using Amnis IDEAS Application v5.0 software. Live BrdU⁺ G₂/M cells were gated, and then phospho-histone H3⁺ cells and multinucleated cells were analyzed in the appropriate gated populations. To quantitate multinucleated cells, guided analysis in the IDEAS software package was used to identify cells with non-round nuclei, and then normal interphase and mitotic cells were manually subtracted.

Immunoblotting. Whole-cell extracts of HeLa cells were prepared using ProteoJET Mammalian Cell Lysis Reagent (Fermentas), followed by denaturation in SDS sample buffer. Proteins were resolved by SDS-PAGE, transferred to nitrocellulose membranes, and then probed with the indicated antibodies. Membranes were developed using the ECL reaction method. The antibodies used include rabbit anti-FANCA (Abcam), rabbit anti-FANCB (Abcam), rabbit anti-FANCC (Abcam), rabbit anti-FANCE (Abcam), mouse anti-FANCG (Abcam), rabbit anti-FANCL (Abcam), mouse anti-FANCD2 (Novus), rabbit anti-FANCI (Abcam), rabbit anti-BRCA2/FANCD1 (Cell Signaling Technology), rabbit anti-PALB2/FANCN (Abcam), mouse anti-RAD51/FANCO (Abcam), rabbit anti-SLX4/FANCP (Abcam), rabbit anti-MAD2 (Santa Cruz), and mouse anti-actin (Sigma-Aldrich) or rabbit anti-GAPDH (Cell Signaling Technology). For immunoblotting of MAD2 in siRNA-knockdown HeLa cells, HeLa cells were transfected with 10 nM siRNA for 48 hours and then whole-

cell extracts were prepared by cell lysis using M-PER Mammalian Protein Extraction Reagent (Thermo Scientific) followed by denaturation in SDS sample buffer. Proteins were resolved by SDS-PAGE, transferred to nitrocellulose membranes, and then probed with rabbit anti-MAD2 (Abcam) and mouse anti-CoxIV (Cell Signaling Technology) or rabbit anti-GAPDH (Cell Signaling Technology). Membranes were developed by quantitative infrared Western blot detection using a LI-COR Odyssey CLx imager.

Quantification of mitotic failure in cells from patients with FA. To assess mitotic spindle checkpoint function in primary patient cells, human skin fibroblasts from patients with FA of 12 different FA complementation groups and from healthy controls were plated at 2×10^5 cells per well on ultrafine coverslips in 6-well plates for 16 hours. Then, the cells were treated with 200 nM taxol for 24 hours and fixed in 4% paraformaldehyde. For imaging, Hoechst 33342 (1 μ g/ml) and Alexa Fluor 594-labeled phalloidin (Invitrogen) were used to stain chromosomes and actin, respectively, and then the coverslips were mounted on glass slides. A DeltaVision deconvolution microscope (Applied Precision) equipped with a $\times 20$ objective was used for image acquisition, and ImageJ was used for quantification of cells. For flow cytometry, cells were permeabilized in 90% methanol for 30 minutes and stained with DRAQ5 DNA stain and an Alexa Fluor 488-conjugated antibody against phospho-histone H3 (Cell Signaling Technology) to identify the mitotic fraction. A BD FACSCalibur flow cytometer and CellQuest Pro software were used for data collection

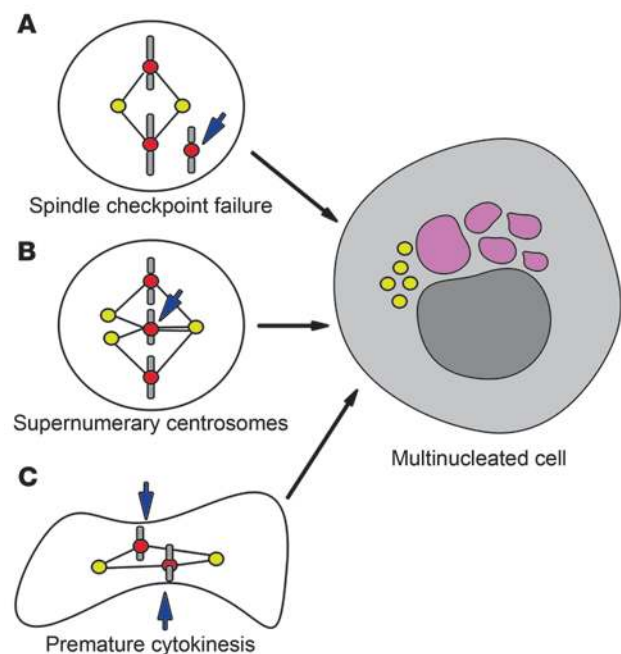


Figure 6

Multiple cell cycle defects may lead to aneuploidy in FA-deficient cells. Loss of the FA signaling pathway results in abnormal mitosis due to **(A)** SAC failure (Figures 1–2); **(B)** presence of supernumerary centrosomes (Figure 5 and Supplemental Figure 11), leading to merotelic kinetochore-spindle attachment, as proposed by Ganem et al. (29); and **(C)** premature cytokinesis, as reported by Vinciguerra et al. (30). The failed mitosis produces multinucleated cells with ongoing mutagenesis in the micronuclei (36). Since FA-deficient cells cannot efficiently recognize and repair DNA damage (reviewed in refs. 1, 2, 43), this process leads to accumulation of mutations and either cell death or malignant transformation. Centrosomes are shown in yellow, kinetochores are shown in red, DNA is shown in gray, and micronuclei undergoing mutagenesis are shown in purple.



and analysis. At least 3 independent experiments were performed for each cell line. The specific mutations detected in the fibroblasts from patients with FA are listed in Supplemental Table 1.

Genetic spindle checkpoint rescue in patient cells. FANCA-deficient patient fibroblasts were transduced with either a retroviral expression construct containing an IRES-NEO cassette or a construct additionally expressing the full-length FANCA cDNA similar to previously described strategies (6, 40, 41). Geneticin was used to select for cells that stably expressed the vector. Cells were grown in the presence of 200 nM taxol or 100 ng/ml nocodazole for 24 hours. Hoechst 33342 (1 µg/ml) and Alexa Fluor 594-labeled phalloidin (Invitrogen) were used to stain chromosomes and actin, respectively, and then the coverslips were mounted on glass slides. A DeltaVision deconvolution microscope (Applied Precision) equipped with a ×20 objective was used for image acquisition, and ImageJ was used for quantification of cells.

Visualization of endogenous FA proteins during mitosis. HeLa cells or HeLa cells stably expressing GFP-CENPA/GFP-γtubulin (38) were grown on ultrathin glass coverslips and extracted in 0.1% Triton X-100 for 2 minutes prior to 10 minute fixation in 4% paraformaldehyde. Cells were further permeabilized in 0.1% Triton X-100 in PBS for 10 minutes after paraformaldehyde fixation. Cells were blocked in 1% BSA or in Image-iT FX signal enhancer for 30 minutes (Invitrogen). See below for the list of primary antibodies used for immunofluorescence. Cells were stained with primary antibodies overnight at 1:100 concentrations in PBS and with fluorescent secondary antibodies (Life Technologies) for 2 hours at 1:10,000 concentrations in PBS. Hoechst 33342 was used to stain DNA. Images were acquired on a DeltaVision deconvolution microscope (Applied Precision) equipped with a ×60 or ×100 objective followed by 10 deconvolution cycles. All images were obtained and processed identically.

List of primary antibodies used for immunofluorescence. The following primary antibodies were used for immunofluorescence: rabbit anti-FANCA (Abcam), rabbit anti-FANCB (Abcam), rabbit anti-FANCC (Abcam), rabbit anti-FANCD2 (Abcam), rabbit anti-FANCE (Abcam), mouse anti-FANCG (Abcam), rabbit anti-BRCA2/FANCD1 (Cell Signaling Technology), rabbit anti-PALB2/FANCN (Abcam), mouse anti-PLK1 (Abcam), and mouse anti-αtubulin (Invitrogen).

Generation and expression of GFP-fused FA proteins. For further visualization of the localization of FA proteins during mitosis, fusion constructs between the EGFP and FANCC, FANCG, or FANCL cDNAs were generated and verified by direct sequencing (C. Marchal and H. Hanenberg, unpublished observations). HeLa cells were reverse transfected with the above constructs using ExGene transfection reagent (Fermentas) at 1×10^5 cells per well on coverslips in 6-well plates. Forty-eight hours after transfection, cells were fixed in 4% paraformaldehyde in PBS. Hoechst 33342 and Alexa Fluor 594-labelled phalloidin (Invitrogen) were used to stain DNA and actin. Coverslips were mounted to ultrathin glass slides, and a DeltaVision deconvolution microscope (Applied Precision) equipped with a ×100 objective was used for image acquisition as described above.

Centrosome visualization and quantification. HeLa cells transfected with siRNAs as described above or human fibroblast cells from patients with FA and healthy controls were fixed in 4% paraformaldehyde, permeabilized in Triton X-100 (Sigma-Aldrich), and blocked in 1% BSA. Immunostaining was performed using a rabbit anti-pericentrin antibody (Abcam). Hoechst 33342 was used to stain DNA. Image acquisition was performed using a DeltaVision deconvolution microscope (Applied Precision) equipped with a ×20 objective. At least 3 experiments were performed for each siRNA or cell line derived from patients with FA.

Statistics. For the siRNA screen, nuclear counts for each siRNA were compared with negative control siRNA by 1-way ANOVA followed by Bonferroni's multiple comparison tests. For taxol-treated patient cell experi-

ments (imaging and flow cytometry) and pericentrin immunofluorescence microscopy experiments (siRNA-transfected HeLa cells and primary fibroblasts from patients with FA), 1-way ANOVA tests were performed followed by Bonferroni's multiple comparison tests to compare each FA sample with the appropriate negative control. For the experiments involving primary fibroblasts from patients with FA, FA cell lines were compared with the average of equal numbers of replicates of 2 healthy control primary fibroblast cell lines. For comparison of MAD2 levels in FANCA siRNA-transfected cells compared with negative control siRNA-transfected cells and quantification of SAC failure in FANCA cells compared with gene-corrected cells as well as CD34⁺ FANCA shRNA-transduced cells compared with negative control CD34⁺ cells, 2-tailed *t* tests were used. *P* values of less than 0.05 were considered significant.

Study approval. Specimens derived from patients with FA were obtained following approval by the local ethics committees (Ethikkommission der Universitaet Wuerzburg, Wuerzburg, Germany and IRB at Rockefeller University, New York, New York, USA). The reference FANCF cell line obtained from Hans Joenje (VU University, Amsterdam, The Netherlands) has previously been published (42). Specimens from patients with FA were obtained from Detlev Schindler (University of Wuerzburg, Wuerzburg, Germany), Hans Joenje (VU University, Amsterdam, The Netherlands), or Arleen Auerbach (The Rockefeller University, New York, New York, USA) in an anonymized fashion.

Acknowledgments

This work was supported by the NIH/NCATS KL2 TR000163 Clinical and Translational Sciences Award, Indiana Pediatric Scientist Award (IPSA) K12, and Morris Green Research Fellowship to G. Nalepa; by the NIH/NCATS TL1 TR000162 Clinical and Translational Sciences Award and NIH/NIGMS GM077229-02 MSTP Award to R. Enzor; by the NIH R01s CA138237-01 and CA155294-01 to D.W. Clapp and H. Hanenberg; and by the BMBF grant "Inherited bone marrow failure syndromes" and DFG SPP1230 to H. Hanenberg. We are grateful to Shaochun Bai (Indiana University, Indianapolis, Indiana, USA) for sequencing the FANCA and FANCC genes in the patient-derived cell lines used in this study, confirming our retroviral complementation studies. We thank Claire Walczak (Indiana University, Bloomington, Indiana, USA) for HeLa cell lines stably expressing GFP-γtubulin/GFP-CENPA and cells stably expressing GFP-H2B/mCherry-αtubulin. We are grateful to H.E. Broxmeyer, E.F. Srour, L.S. Haneline, and D.A. Ingram (all at Indiana University School of Medicine, Indianapolis, Indiana, USA) for critical reading of the manuscript. We thank D. Schindler (University of Wuerzburg, Wuerzburg, Germany) for sharing unpublished mutations that confirmed our retroviral complementation results. We thank the patients with FA and families, Fanconi Anemia Research Fund Inc., and German family organizations "Aktionskreis FA e.V." and "Deutsche FA Hilfe e.V." for their support of our research. We acknowledge the In Vivo Therapeutics Core of Indiana University Simon Cancer Center as well as Arthur Baluyut (St. Vincent Hospital, Indianapolis, Indiana, USA) for umbilical cord blood samples. Indiana University is a Center for Excellence in Molecular Hematology (P30).

Received for publication October 24, 2012, and accepted in revised form May 30, 2013.

Address correspondence to: D. Wade Clapp, Indiana University School of Medicine, Herman B Wells Center for Pediatric Research, 1044 W. Walnut Street, R4-402, Indianapolis, Indiana 46202, USA.



Phone: 317.278.9290; Fax: 317.274.0138; E-mail: dclapp@iu.edu. Or to: Grzegorz Nalepa, Indiana University School of Medicine, Department of Pediatrics, Division of Pediatric Hematology-Oncology, Herman B Wells Center for Pediatric Research, 1044 W. Walnut Street, R4-421, Indianapolis, Indiana 46202, USA. Phone: 317.278.9846; Fax: 317.274.0138; E-mail: gnalepa@iu.edu.

1. D'Andrea AD. The Fanconi road to cancer. *Genes Dev.* 2003;17(16):1933–1936.
2. D'Andrea AD. Susceptibility pathways in Fanconi's anemia and breast cancer. *N Engl J Med.* 2010; 362(20):1909–1919.
3. de Winter JP, Joenje H. The genetic and molecular basis of Fanconi anemia. *Mutat Res.* 2009; 668(1–2):11–19.
4. Alter BP, et al. Malignancies and survival patterns in the National Cancer Institute inherited bone marrow failure syndromes cohort study. *Br J Haematol.* 2010;150(2):179–188.
5. Crossan GP, Patel KJ. The Fanconi anaemia pathway orchestrates incisions at sites of crosslinked DNA. *J Pathol.* 2012;226(2):326–337.
6. Meindl A, et al. Germline mutations in breast and ovarian cancer pedigrees establish RAD51C as a human cancer susceptibility gene. *Nat Genet.* 2010; 42(5):410–414.
7. Rahman N, et al. PALB2, which encodes a BRCA2-interacting protein, is a breast cancer susceptibility gene. *Nat Genet.* 2007;39(2):165–167.
8. Reid S, et al. Biallelic mutations in PALB2 cause Fanconi anemia subtype FA-N and predispose to childhood cancer. *Nat Genet.* 2007;39(2):162–164.
9. Seal S, et al. Truncating mutations in the Fanconi anemia J gene BRIP1 are low-penetrance breast cancer susceptibility alleles. *Nat Genet.* 2006; 38(11):1239–1241.
10. Jones S, et al. Exomic sequencing identifies PALB2 as a pancreatic cancer susceptibility gene. *Science.* 2009; 324(5924):217.
11. Pennington KP, Swisher EM. Hereditary ovarian cancer: beyond the usual suspects. *Gynecol Oncol.* 2012;124(2):347–353.
12. Turnbull C, Rahman N. Genetic predisposition to breast cancer: past, present, and future. *Annu Rev Genomics Hum Genet.* 2008;9:321–345.
13. Berger R, Le Coniat M, Schaison G. Chromosome abnormalities in bone marrow of Fanconi anemia patients. *Cancer Genet Cytogenet.* 1993;65(1):47–50.
14. Mehta PA, et al. Numerical chromosomal changes and risk of development of myelodysplastic syndrome – acute myeloid leukemia in patients with Fanconi anemia. *Cancer Genet Cytogenet.* 2010; 203(2):180–186.
15. Tutt A, et al. Absence of Brca2 causes genome instability by chromosome breakage and loss associated with centrosome amplification. *Curr Biol.* 1999; 9(19):1107–1110.
16. Kim H, D'Andrea AD. Regulation of DNA cross-link repair by the Fanconi anemia/BRCA pathway. *Genes Dev.* 2012;26(13):1393–1408.
17. Lara-Gonzalez P, Westhorpe FG, Taylor SS. The spindle assembly checkpoint. *Curr Biol.* 2012;22(22):R966–R980.
18. Musacchio A, Salmon ED. The spindle-assembly checkpoint in space and time. *Nat Rev Mol Cell Biol.* 2007;8(5):379–393.
19. Chan KL, Palmal-Pallag T, Ying S, Hickson ID. Replication stress induces sister-chromatid bridging at fragile site loci in mitosis. *Nat Cell Biol.* 2009; 11(6):753–760.
20. Naim V, Rosselli F. The FANCD1/BLM collaborate during mitosis to prevent micro-nucleation and chromosome abnormalities. *Nat Cell Biol.* 2009; 11(6):761–768.
21. Berger R, Bernheim A, Le Coniat M, Vecchione D, Schaison G. Chromosomal studies of leukemic and preleukemic Fanconi's anemia patients: examples of acquired 'chromosomal amplification.' *Hum Genet.* 1980;56(1):59–62.
22. Willingale-Theune J, Schweiger M, Hirsch-Kauffmann M, Meek AE, Paulin-Levasseur M, Traub P. Ultrastructure of Fanconi anemia fibroblasts. *J Cell Sci.* 1989;93(pt 4):651–665.
23. Malul SW, Erdtmann B. Genomic instability in Down syndrome and Fanconi anemia assessed by micronucleus analysis and single-cell gel electrophoresis. *Cancer Genet Cytogenet.* 2001;124(1):71–75.
24. Pulliam-Leath AC, et al. Genetic disruption of both Fancd1 and Fancg in mice recapitulates the hematopoietic manifestations of Fanconi anemia. *Blood.* 2010;116(16):2915–2920.
25. Nalepa G, et al. The tumor suppressor CDKN3 controls mitosis. *J Cell Biol.* 2013;201(7):997–1012.
26. Stegmeier F, et al. Anaphase initiation is regulated by antagonistic ubiquitination and deubiquitination activities. *Nature.* 2007; 446(7138):876–881.
27. Sigoillot FD, et al. A bioinformatics method identifies prominent off-targeted transcripts in RNAi screens. *Nat Methods.* 2012;9(4):363–366.
28. Rosenberg PS, Greene MH, Alter BP. Cancer incidence in persons with Fanconi anemia. *Blood.* 2003; 101(3):822–826.
29. Ganem NJ, Godinho SA, Pellman D. A mechanism linking extra centrosomes to chromosomal instability. *Nature.* 2009;460(7252):278–282.
30. Vinciguerra P, Godinho SA, Parmar K, Pellman D, D'Andrea AD. Cytokinesis failure occurs in Fanconi anemia pathway-deficient murine and human bone marrow hematopoietic cells. *J Clin Invest.* 2010; 120(11):3834–3842.
31. Gordon DJ, Resio B, Pellman D. Causes and consequences of aneuploidy in cancer. *Nat Rev Genet.* 2012; 13(3):189–203.
32. Kupfer GM, Yamashita T, Naf D, Suliman A, Asano S, D'Andrea AD. The Fanconi anemia polypeptide, FAC, binds to the cyclin-dependent kinase, cdc2. *Blood.* 1997;90(3):1047–1054.
33. Mi J, et al. FANCD1 is phosphorylated at serines 383 and 387 during mitosis. *Mol Cell Biol.* 2004; 24(19):8576–8585.
34. D'Angiello V, Mari C, Nocera D, Rametti L, Grieco D. The spindle checkpoint requires cyclin-dependent kinase activity. *Genes Dev.* 2003; 17(20):2520–2525.
35. Lee H, et al. Mitotic checkpoint inactivation fosters transformation in cells lacking the breast cancer susceptibility gene, Brca2. *Mol Cell.* 1999;4(1):1–10.
36. Crasta K, et al. DNA breaks and chromosome pulverization from errors in mitosis. *Nature.* 2012; 482(7383):53–58.
37. Stephens PJ, et al. Massive genomic rearrangement acquired in a single catastrophic event during cancer development. *Cell.* 2011;144(1):27–40.
38. Cai S, O'Connell CB, Khodjakov A, Walczak CE. Chromosome congression in the absence of kinetochore fibres. *Nat Cell Biol.* 2009;11(7):832–838.
39. Cai S, Weaver LN, Ems-McClung SC, Walczak CE. Proper organization of microtubule minus ends is needed for midzone stability and cytokinesis. *Curr Biol.* 2010;20(9):880–885.
40. Vaz F, et al. Mutation of the RAD51C gene in a Fanconi anemia-like disorder. *Nat Genet.* 2010; 42(5):406–409.
41. Antonio Casado J, et al. A comprehensive strategy for the subtyping of patients with Fanconi anaemia: conclusions from the Spanish Fanconi Anemia Research Network. *J Med Genet.* 2007; 44(4):241–249.
42. de Winter JP, et al. The Fanconi anaemia gene FANCF encodes a novel protein with homology to ROM. *Nat Genet.* 2000;24(1):15–16.
43. Grompe M, D'Andrea A. Fanconi anemia and DNA repair. *Hum Mol Genet.* 2001;10(20):2253–2259.